

Supporting Information: Unified approach to implicit and explicit solvent simulations of electrochemical reaction energetics

Joseph A. Gauthier,^{†,‡} Colin F. Dickens,^{†,‡} Hendrik H. Heenen,[¶] Sudarshan Vijay,[¶] Stefan Ringe,^{‡,†} and Karen Chan^{*,¶}

[†]*SUNCAT Center for Interface Science and Catalysis, Department of Chemical Engineering, Stanford University, Stanford, California 94305, United States*

[‡]*SUNCAT Center for Interface Science and Catalysis, SLAC National Accelerator Laboratory, 2575 Sand Hill Road, Menlo Park, California 94025, United States*

[¶]*Department of Physics, Technical University of Denmark, DK-2800, Kgs. Lyngby, Denmark*

E-mail: kchan@fysik.dtu.dk

Note 1

In this note, we further explain the use of the average work function, $\bar{\Phi}$, as the descriptor for electrochemical reactions used in the main text.

In the main text, we establish that the energy depends quadratically on the surface charge density q and the potential Φ . That is, we assume that the capacitance is a constant function of potential and therefore the cubic term in the Taylor expansion is negligible (this is shown to be a good assumption in Figure 4). Expanding the energy as a function of q , we have

$$E(q) = E(q = 0) + q\Phi_0 + \frac{q^2}{2C} . \quad (\text{S1})$$

We can write this instead as a function of potential by using the usual capacitance relation $q = C(\Phi - \Phi_0)$,

$$E(\Phi) = E(\Phi = \Phi_0) + C\Phi_0(\Phi - \Phi_0) + \frac{C}{2}(\Phi - \Phi_0)^2 . \quad (\text{S2})$$

Seen in Figure S1 is a plot of the energy E as a function of the coverage θ of (in this case) protons. In general, the energy depends quadratically on both θ and work function Φ .¹ In practical density functional theory (DFT) calculations of relative energies between two different states of θ or Φ , the change in energy calculated is not equal to $dE/d\theta$. Instead it is equal to $\Delta E/\Delta\theta$, since the coverage changes substantially between the initial and final state. This is illustrated in Figure S1, where the blue dashed line indicates the energy change between two DFT calculations with different coverages (theta=0 and 0.5). What one would like to calculate though is instead the instantaneous derivative, in order to relate energy differences to a coverage or work function. Toward this end, we take advantage of a property of parabolas, for which the slope of a secant line is equivalent to the slope of the tangent at the average value of the independent variable. For a general parabola $f(x) = c_1x^2 + c_2x + c_3$,

the slope of a secant line from point a to b is given by

$$\begin{aligned}
 \frac{\Delta f(x)}{\Delta x} &= \frac{f(b) - f(a)}{b - a} \\
 &= \frac{c_1(b^2 - a^2) + c_2(b - a)}{b - a} \\
 &= c_1(b + a) + c_2 \quad .
 \end{aligned} \tag{S3}$$

The slope of the tangent line at a given point x is then given by

$$\frac{df}{dx} = 2c_1x + c_2 \quad . \tag{S4}$$

Equating (S3) and (S4), we see that the slope of the tangent line and secant line are equivalent for the tangent to the average of a and b , i.e.

$$\frac{df}{dx}(x = \frac{a+b}{2}) = \frac{f(b) - f(a)}{b - a} \quad . \tag{S5}$$

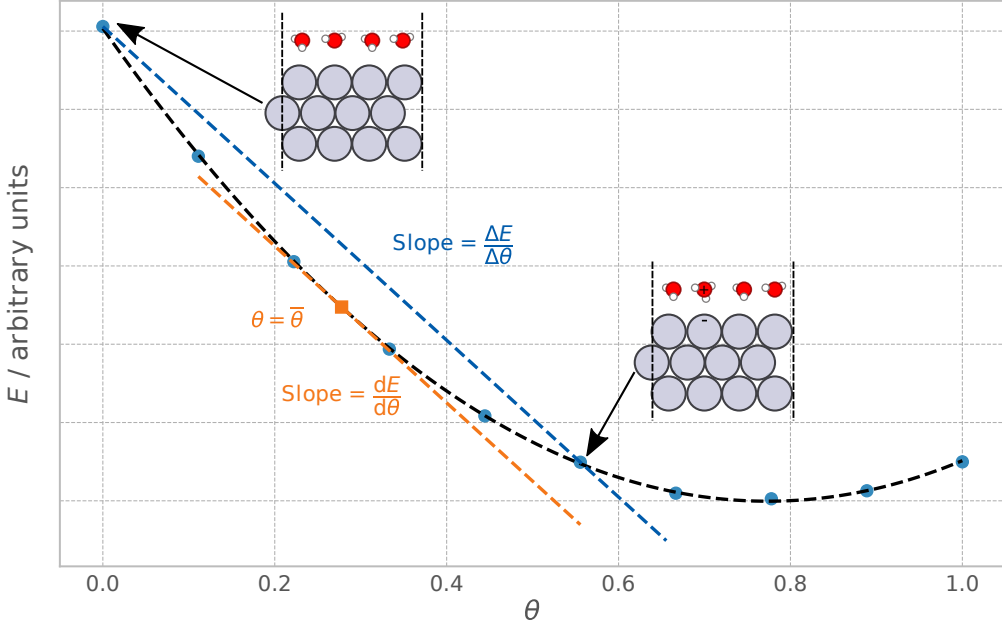


Figure S1: Graphic explanation of the average work function being used to describe reaction energetics. In this graphic, the coverage of protons θ is used to illustrate the concept. Since the energy E depends quadratically on θ , the slope of the secant line between two points θ_1 and θ_2 is exactly equal to the slope of the tangent line at $\theta = \bar{\theta}$.

In the context of Figure S1, this means that the change in energy calculated between two states in a standard DFT calculation (in the Figure, going from $\theta = 0$ to $\theta = 0.5$) is equivalent to the DFT calculation with no change in coverage between initial and final states (i.e. cell-extrapolated), at a coverage of $\theta = \bar{\theta} = 0.25$.

Because the energy also depends quadratically on the work function Φ , the same argument is made. The change in energy as calculated by DFT in a finite cell, which results in a change in work function $\Phi_1 \rightarrow \Phi_2$, is exactly equivalent to the calculation with no change in work function, at the average work function. By analogy to Eq. (S5),

$$\frac{dE}{d\theta}(\theta = \bar{\theta}) = \frac{E(\theta_2) - E(\theta_1)}{\theta_2 - \theta_1} \quad (S6)$$

$$\frac{dE}{d\Phi}(\Phi = \bar{\Phi}) = \frac{E(\Phi_2) - E(\Phi_1)}{\Phi_2 - \Phi_1} \quad . \quad (S7)$$

Note 2

Here we illustrate a third example of surface charge as the descriptor for the driving force of charge transfer processes. Shown in Figure S2 is the binding energy of two CO₂ molecules as both a function of the average work function, and as a function of the average effective charge. Note that the binding energy for two CO₂ molecules is shown because a cell symmetric in the z -coordinate was used.

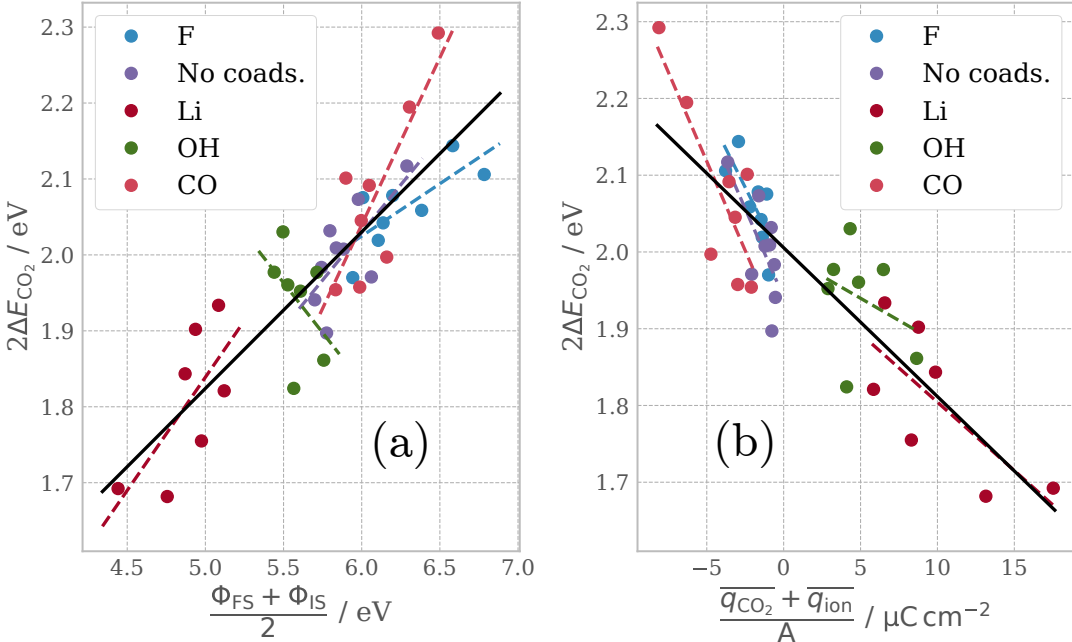


Figure S2: Binding energy of CO₂ on Pt (111) with various coadsorbates to modify the work function. (a) ΔE_{CO_2} as a function of the average work function. (b) ΔE_{CO_2} as a function of the effective surface charge. The solid black line represents a best fit to all data points.

As can be seen in Figure S2(a), the data shows a significant amount of noise. This is due largely to the chemical interaction between the coadsorbate and CO₂ on the surface. We note that the scale on the y-axis is rather small, and so the average deviation remains quite small overall. Figure S2(b) shows some reduced noise, with all slopes having the same sign. As outlined in the main text, the effective charge q_{eff} , due to the ion (and CO₂) is determined via

$$q_{\text{eff}} = \frac{\partial \Delta E_{\text{ion}}}{\partial \bar{\Phi}} . \quad (\text{S8})$$

Note 3

In this note, we discuss tuning the capacitance of the implicit model, such that it matches that of the overall process. In principle this would mitigate the issues presented in the main text, where the work function acts as a poor descriptor for the driving force. If the capacitance for every charging process in the system is the same, then the work function can act as a descriptor. We found that using a partial bilayer of explicit solvent (rather than a full bilayer), equivalent to only one water molecule to stabilize each hydronium ion, lowered the capacitance due to explicit protons.

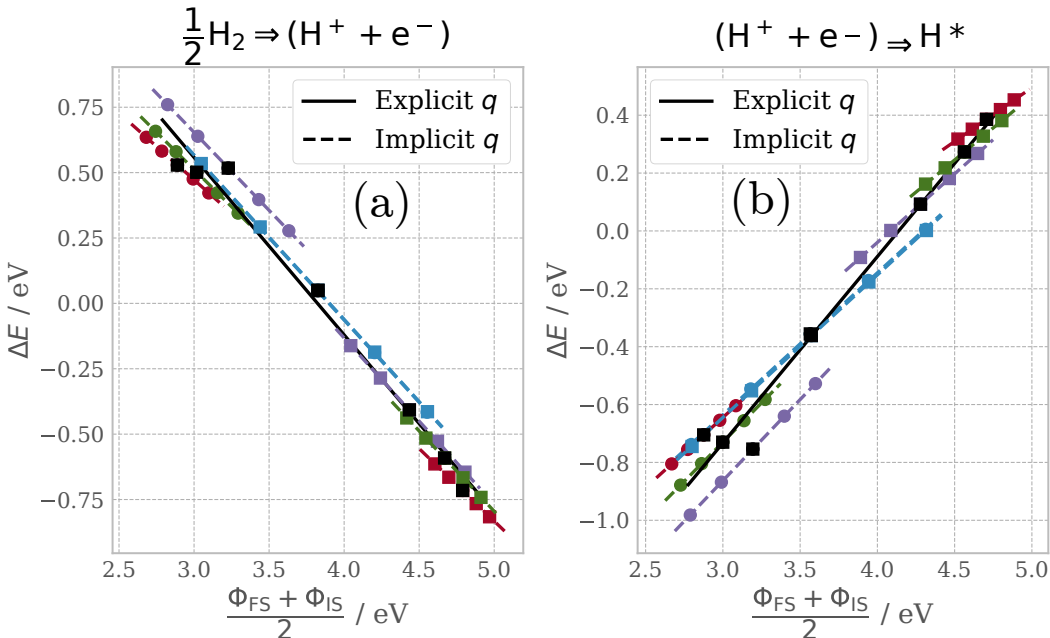


Figure S3: Illustration of capacitance tuning for (a) proton creation and (b) the Volmer reaction. Here the dashed colored lines correspond to different fixed proton concentrations, with the work function being modified by changing the continuum countercharge. The dashed line corresponds to the case of zero continuum countercharge, with the work function being modified by changing the explicit proton coverage (i.e. cell extrapolation).

As can be seen in Figure S3, using a very sparse bilayer sufficiently lowers the capacitance of explicit charging, to the point that it roughly matches that of implicit charging. This results in the work function acting as a better descriptor for the driving force, as evidenced by the lines for implicit and explicit charging being approximately parallel and having similar intercepts. Figure S4 illustrates the problem with this approach of tuning the capacitance.

Here we plot the Volmer reaction energy as a function of (a) the proton coverage θ and (b) work function Φ .

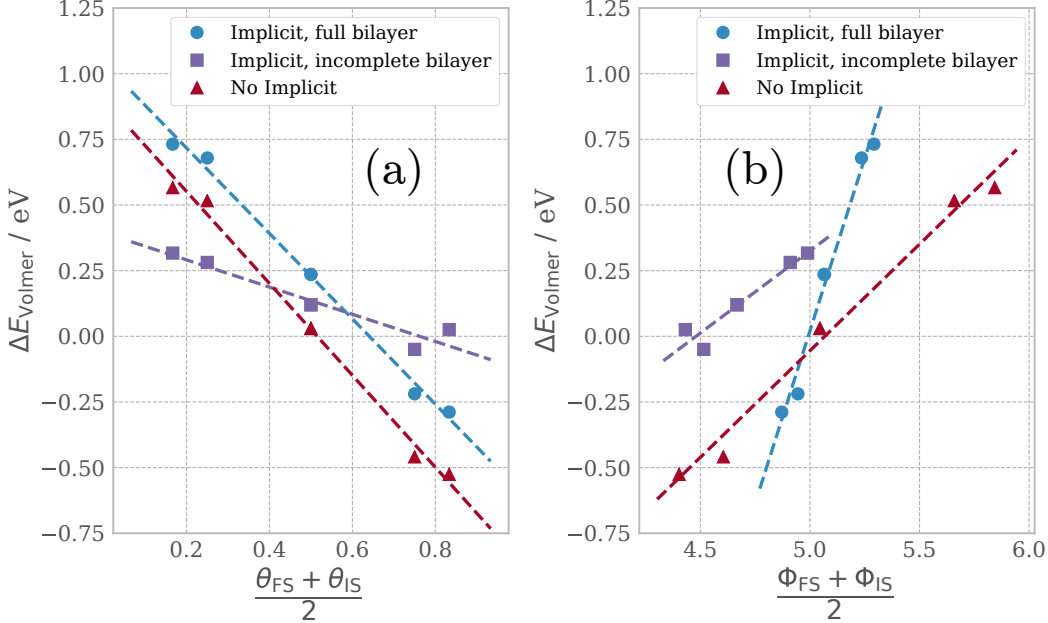


Figure S4: Illustration of the problem using an incomplete bilayer to tune the capacitance. (a) Change in Volmer reaction energy as a function of the coverage of protons. (b) Change in Volmer reaction energy as a function of the work function. With an incomplete bilayer, $\partial \Delta^2 E_{\text{Volmer}} / \partial \bar{\Phi}^2$ is equivalent to the case with no implicit solvent, indicating equivalent capacitance. However, $\partial^2 \Delta E_{\text{Volmer}} / \partial \bar{\theta}^2$ is significantly reduced with the incomplete bilayer, indicating a reduced proton-proton interaction.

As we showed earlier in Note 1, the points in the above plots are exactly equivalent to the instantaneous derivatives. That is, the points in Figure S4(a) correspond to $\partial E / \partial \theta$, while the points in Figure S4(b) correspond to $\partial E / \partial \Phi$, and therefore the slope of the lines correspond to $\partial^2 E / \partial \theta^2$ and $\partial^2 E / \partial \Phi^2$ respectively. Using the chain rule, we can write

$$\frac{\partial^2 E}{\partial \Phi^2} = \frac{\partial^2 E}{\partial \theta^2} \left(\frac{\partial \theta}{\partial \Phi} \right)^2 \quad (\text{S9})$$

In a 6x3 supercell of Pt (111), we calculated from DFT the change in work function upon the removal of a proton from the water bilayer (i.e. via the Volmer reaction), tabulated in Table S1.

Table S1: Calculated changes in work function across Volmer reaction coordinate in a 6x3 supercell of Pt (111)

Case	$\Delta\Phi$ / eV
Implicit, full bilayer	0.26
Implicit, incomplete bilayer	0.32
No implicit, full bilayer	0.79
No implicit, incomplete bilayer	0.84

Because the cell size is the same for each of these cases, these numbers can be used as approximations to a number proportional to the inverse of the instantaneous proton dipole moment, $\partial\theta/\partial\Phi$,

$$\frac{\partial\Phi}{\partial\theta} \propto \Delta\Phi \quad (\text{S10})$$

Returning to Figure S4(b), we can see that the slope of the line corresponding to an incomplete bilayer is the same as that of the case with no continuum solvation, which explains the reasonable agreement in Figure S3. However, as seen in Figure S4(a) since the slope of the line corresponding to an incomplete bilayer is different than the other cases, this means that using an incomplete bilayer changes $\partial^2E/\partial\theta^2$, which represents the proton-proton interaction. In other words, while the use of an incomplete bilayer does in fact change the capacitance in a way that allows the work function to be used as the descriptor, it does so by decreasing the interaction between protons, i.e. the explicit capacitance.

Ideally, the capacitance would instead be tuned the other way, without affecting the proton-proton interaction and instead increasing the capacitance associated with continuum charging. This in principle could be done by for example changing the parameters built into the continuum model. However this would necessarily affect other factors in the system, such as the solvation energy. It would also not be easily generalizable to new systems, and would have to be fit for each case, limiting its use in practice.

Finally, we now show that by adjusting the parameters of the solvation model, using Quantum-Espresso/Environ and its solvent aware technology,² the predicted effective charge can approach the expected value from previous studies using a capacitor model of the inter-

face or charge partitioning, illustrated in Figure S5.

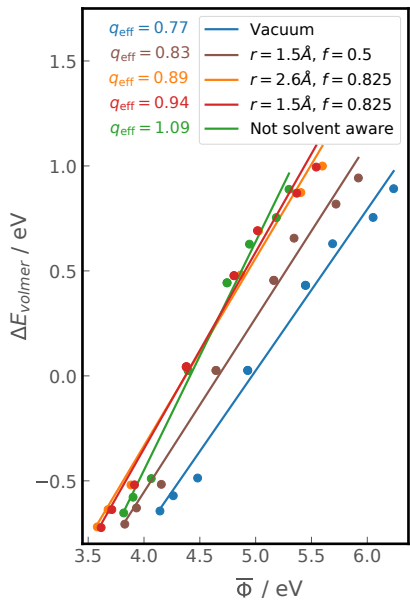


Figure S5: Illustration of the calculated effective charge associated with the Volmer reaction. The solvent aware technology of Environ has two tunable parameters: the solvent radius, r , and the filling threshold, f . Further details can be found in Environ's documentation.

Note 4

Here we expand upon the methods used to generate the data found in Figure 7 in the main text.

In Figure S6, we show the Volmer reaction energy, with no continuum solvation, for varying water structures at each point.

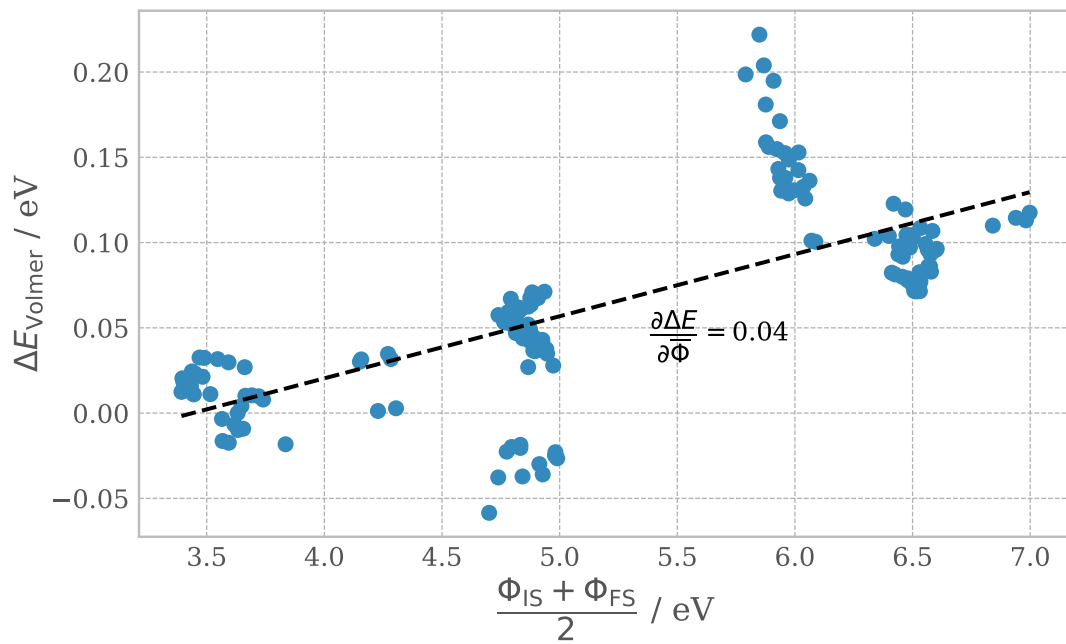


Figure S6: Volmer reaction energy as a function of work function for approximately 100 different water structures. The first water bilayer is identical for each point, while the three layers above change for each point. Despite a more than 3 eV change in the work function, the range of Volmer reaction energies varies by less than 0.3 eV.

As can be seen in Figure S6, there is a wide range of work function and yet only a small range of energies. The small amount of scatter is likely due to very slightly different water structures between initial and final state. The picture in this system is directly analogous to the Frumkin correction, where only the potential drop between the electrode and the inner Helmholtz plane (IHP) contributes to the electron transfer driving force. Here, only the potential drop between the electrode and the first solvent bilayer contributes to the reaction driving force; the changes in measured work function convolute this potential drop and the potential drop due to water dipoles. This results in a huge variation of work function, but with very little change in driving force.

To generate the different water structures, the first water bilayer and the entire Pt (111) slab were fixed, and the top three water bilayers then underwent 5 picoseconds of ab-initio molecular dynamics (AIMD). A Nosé thermostat (IBRION = 0, SMASS = 3) was used to control the temperature, with a set point of 300 K, and a time-step of 1 picosecond (POTIM = 1.). Van der Waals interactions were accounted for using the damped DFT-D3 correction of Grimme^{3,4} (IVDW = 11). From the MD trajectory, snapshots were taken every 20 femtoseconds. The water structure in the top three layers was relaxed above the initial and final state of the Volmer reaction, where the first bilayer was fixed to avoid chemical effects convoluting the energetics. This then gives approximately 250 Volmer reaction energies, each with a different water structure. The mean square displacement between the initial and final state were calculated illustrated in Figure S7.

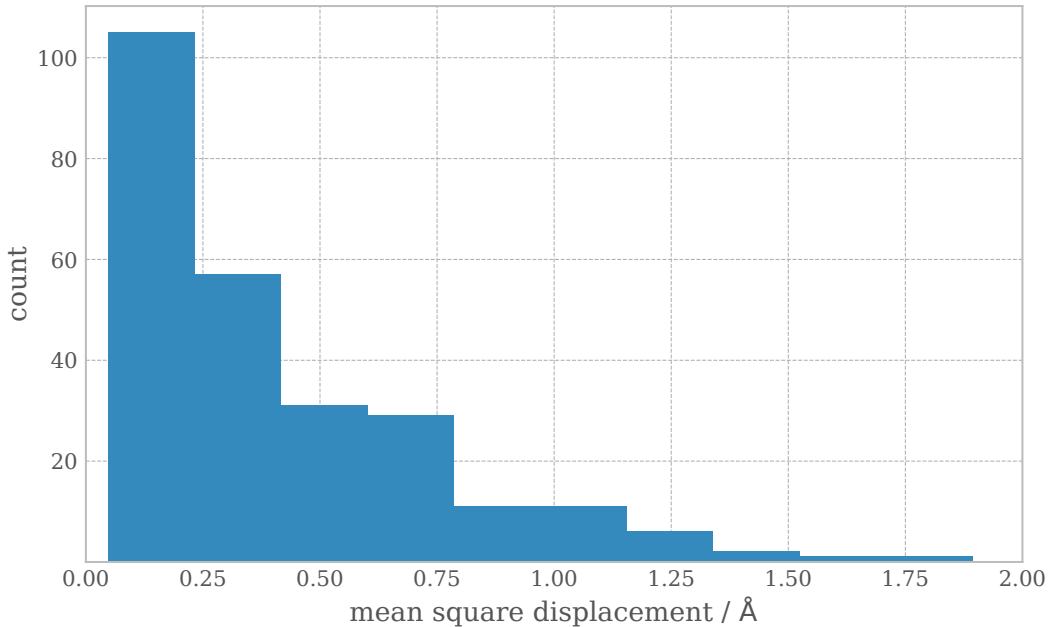


Figure S7: Histogram illustrating the mean square displacement between initial and final states for the 254 Volmer reaction energies calculated.

The purpose of this exercise is to illustrate that, when holding chemical effects (e.g. hydrogen bonding, solvation) constant, the contribution of the changed water structure to the driving force of the reaction is negligible. To this end we did not include the energies associated with any water structure where the initial state and final state differed by a mean square displacement of greater than 0.5 Å. We note that including all trajectories does not significantly change the slope of the line shown in Figure 7 in the main text, going from 0.036 to 0.047 by including every water structure. However, the range of energies (that is, the highest ΔE_{Volmer} minus the lowest ΔE_{Volmer}) does change somewhat, illustrated in Figure S8. This can be explained by the change in water structure between initial and final state causing a change in the chemical effects we presume to be constant.

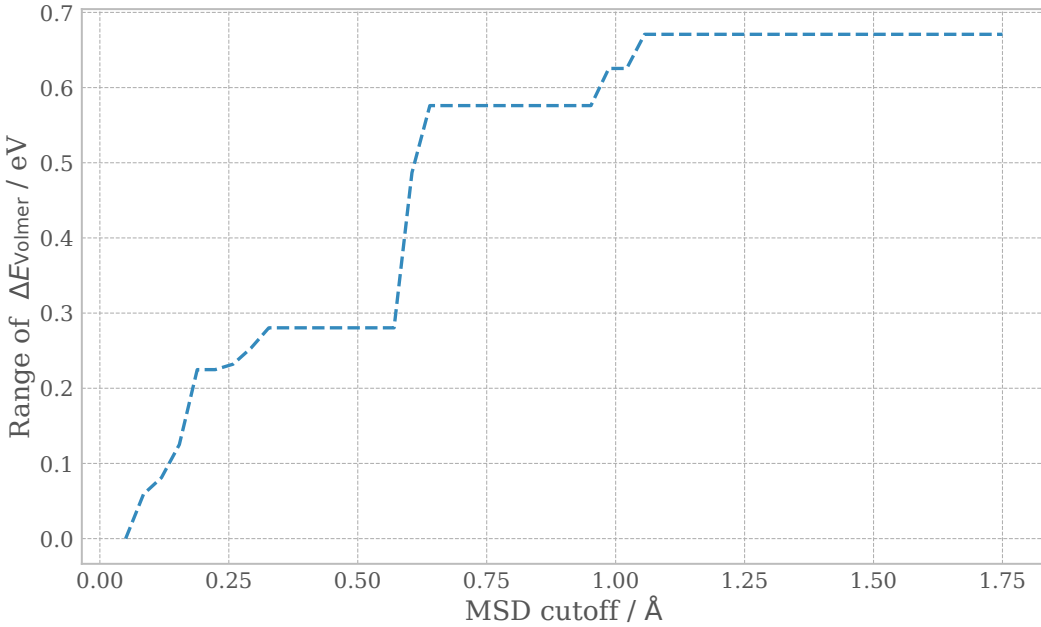


Figure S8: Range of energies (highest ΔE_{Volmer} minus lowest ΔE_{Volmer}) as a function of the cutoff mean square displacement.

Note 5

Here we show the capacitance curves associated with our illustration that the reaction energetics are insensitive to the countercharge placement model chosen. Figure S9 illustrates that the capacitance can change somewhat significantly, which corresponds to a significant difference in energetics as a function of potential.

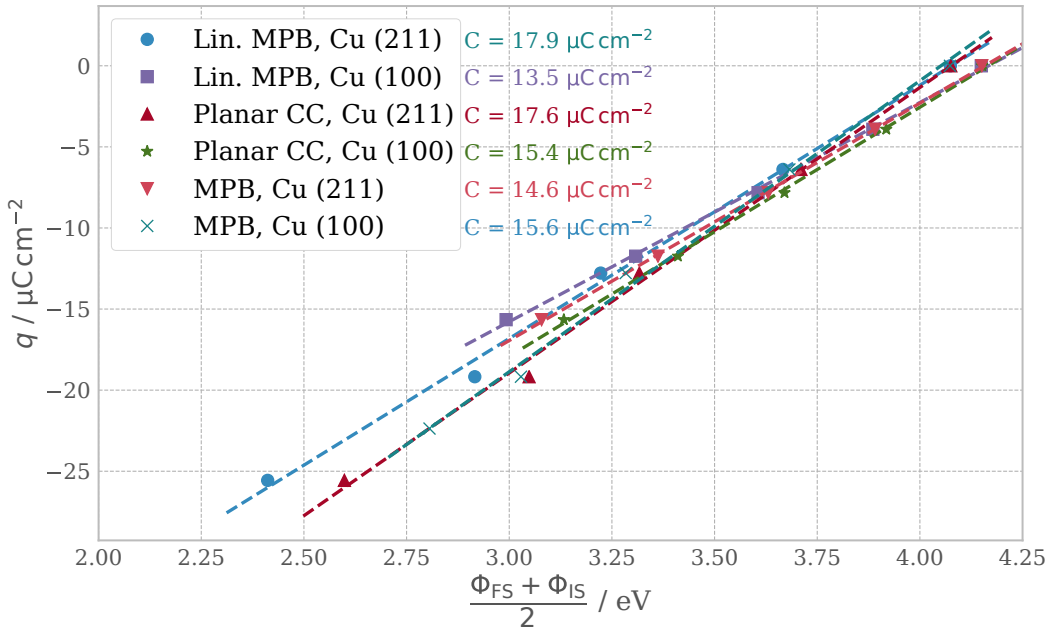


Figure S9: Capacitance curves for Cu (211) and Cu (100) with three charge placement models: the modified Poisson-Boltzmann (MPB) and its linearized version (LMPB) and a planar counter-charge (PCC).

References

- (1) Mamatkulov, M.; Filhol, J.-S. An ab initio study of electrochemical vs. electromechanical properties: the case of CO adsorbed on a Pt(111) surface. *Physical chemistry Chemical Physics : PCCP* **2011**, *13*, 7675–7684.
- (2) Andreussi, O.; Hormann, N. G.; Nattino, F.; Fisicaro, G.; Goedecker, S.; Marzari, N. Solvent-aware interfaces in continuum solvation. *Journal of chemical theory and computation* **2019**,
- (3) Grimme, S.; Antony, J.; Ehrlich, S.; Krieg, H. A consistent and accurate ab initio parametrization of density functional dispersion correction (DFT-D) for the 94 elements H-Pu. *The Journal of Chemical Physics* **2010**, *132*, 154104.
- (4) Grimme, S.; Ehrlich, S.; Goerigk, L. Effect of the damping function in dispersion cor-

rected density functional theory. *Journal of Computational Chemistry* **2011**, *32*, 1456–1465.

Tables and data corresponding to figures from the main text

Here we provide tables and input files necessary to reproduce all figures from the main text.

0.0.1 Figures 1-3

The data used in the plots of Figure 1 have deliberately arbitrary units and so no values are provided. Figures 2 and 3 are similarly explanatory schematics with no data to provide.

0.0.2 Figure 4

Data corresponding to Figure 4:

E / eV	q / $\mu\text{C cm}^{-2}$	Φ / eV
3.59217955516	-34.8284051634	6.54577080861
2.94602229419	-29.0236709695	6.37106408838
1.11745081766	-11.6094683878	5.79784938832
0.547778509728	-5.80473419391	5.58565829728
0.0	0.0	5.36309412301
-0.524280672303	5.80473419391	5.13279412303
-1.02469150461	11.6094683878	4.89749412305
-2.37164365156	29.0236709695	4.09759412312
-2.76694917388	34.8284051634	3.82759412314

Geometry input (POSCAR):

Pt
1.000000000000000
5.6416157967247482 0.000000000000000 0.000000000000000
-2.8208078983623746 4.8857825983552177 0.000000000000000
0.000000000000000 0.000000000000000 16.9312444075633444

Pt

16

Selective dynamics

Direct

0.0000000000000000 0.0000000000000000 0.2953120207612443 T T T
0.333333333333357 0.1666666666666643 0.4319843258704026 F F F
0.1666666666666643 0.333333333333357 0.5680156741295903 F F F
0.5000000000000000 0.0000000000000000 0.7046879792387557 T T T
0.0000000000000000 0.5000000000000000 0.2953120207612443 T T T
0.333333333333357 0.6666666666666643 0.4319843258704026 F F F
0.1666666666666643 0.833333333333357 0.5680156741295903 F F F
0.5000000000000000 0.5000000000000000 0.7046879792387557 T T T
0.5000000000000000 0.0000000000000000 0.2953120207612443 T T T
0.833333333333357 0.1666666666666643 0.4319843258704026 F F F
0.6666666666666643 0.333333333333357 0.5680156741295903 F F F
0.0000000000000000 0.0000000000000000 0.7046879792387557 T T T
0.5000000000000000 0.5000000000000000 0.2953120207612443 T T T
0.833333333333357 0.6666666666666643 0.4319843258704026 F F F
0.6666666666666643 0.833333333333357 0.5680156741295903 F F F
0.0000000000000000 0.5000000000000000 0.7046879792387557 T T T

VASP input file (INCAR):

INCAR created by Atomic Simulation Environment

ENCUT = 500.00000

SIGMA = 0.050000

EDIFF = 0.0001

EDIFFG = -0.03

PREC = Accurate

GGA = RP

ALGO = Normal

ISMEAR = 0

NELM = 250

NSW = 1000

IBRION = 2

NCORE = 16

KPAR = 7

LVHAR = .TRUE.

POTIM = 0.2

LSOL = .TRUE.

LAMBDA_D_K = 3.0

TAU = 0

NELECT = 160.0

Note that for different charges, the entry "NELECT" was varied to produce the different data points.

Figure 5

Data corresponding to Figure 5:

$\Delta E_{\text{CO}_2} / \text{eV}$	$\overline{\Phi} / \text{eV}$
0.792935455	6.28890967801
0.770970825	5.97826231432
0.738200705	5.88380788214
0.74461845	5.89182506158
0.738964705	5.83729891305
0.75026978	5.79672813601

0.726125725	5.7424552028
0.70478197	5.69967657212
0.72697721	5.69418021333

$\Delta E_{\text{Volmer}} / \text{eV}$	$\overline{\Phi} / \text{eV}$
0.007504865	4.89874704757
0.007504865	4.89874704757
0.41209548	5.40688860091
0.41209548	5.40688860091
-0.49698839	4.45877079266
0.61101113	5.71845917931
-0.569108955	4.25263910041
0.72221029	6.05602074766
-0.6297205	4.0919129468
0.865047195	6.2688255888

INCAR file used for all relaxations:

INCAR created by Atomic Simulation Environment

ENCUT = 500.000000

SIGMA = 0.050000

EDIFF = 1.00e-04

EDIFFG = -3.00e-02

PREC = Accurate

GGA = RP

ALGO = Normal

ISMEAR = 0

NELM = 250

IBRION = 2

NSW = 1000

NCORE = 8

LCHARG = .FALSE.

LVHAR = .TRUE.

POTIM = 0.2

Figure 6

Data corresponding to Figure 6:

ΔE_{CO_2} / eV	$\bar{\Phi}$ / eV	$\frac{\overline{q}_{\text{exp}} + \overline{q}_{\text{imp}}}{A}$ / $\mu\text{C cm}^{-2}$
0.828276295904	6.49583282309	-18.98422594965748
0.759159431139	6.14206438771	-13.187515736021604
0.68698319	5.73174670785	-7.390805522385735
0.609809068873	5.28659732377	-1.5940953087498642
0.527712109267	4.80426334468	4.202614904886007
0.662830706404	5.63750003294	-4.218716877701725
0.64629998524	5.54816033602	-2.93055905244929
0.63054565	5.4486691568	-1.6424012271968547
0.613580105537	5.35092466013	-0.3542434019444195
0.596162021355	5.25031003708	0.9339144233080157
0.655021204929	5.66675165168	-4.752626121260275
0.637691037627	5.5608497206	-3.3014425727838552
0.61988995	5.45249300547	-1.850259024307435
0.601384484698	5.34162941458	-0.3990754758310153
0.5823098632	5.22829286981	1.0521080726454044
0.628624848854	5.56851868627	-3.164037658276294
0.616748694948	5.49756931374	-2.1979192893369675

0.604670905	5.42467993696	-1.2318009203976412
0.592208413022	5.35143035821	-0.2656825514583149
0.579540496008	5.2759801734	0.7004358174810115
0.622193209356	5.50065365697	-2.1093584388508626
0.610934092943	5.45866764064	-1.465279526224645
0.603850005	5.40769888684	-0.8212006135984273
0.595544993331	5.3583025981	-0.17712170097220975
0.587245114004	5.30774025542	0.46695721165400783
0.671657481053	5.75010709701	-6.328075316552487
0.646179401271	5.6041674754	-4.395838578673864
0.621835495	5.47060795729	-2.4636018407952425
0.591609087227	5.32983210385	-0.5313651029166206
0.56354714075	5.1830535637	1.4008716349620012
0.593897902674	5.6049490798	-3.996679147296306
0.57678212967	5.51764258813	-2.7763191023203344
0.56015639	5.43087294754	-1.5559590573443633
0.543429494099	5.34125882391	-0.33559901236839207
0.526641696634	5.25017264956	0.8847610326075792
0.605771838073	5.52015123547	-2.8124779184677715
0.592672531753	5.45641443438	-1.9537060349661615
0.58310706	5.39182693452	-1.094934151464552
0.566062275784	5.32740140522	-0.23616226796294246
0.55243641026	5.26183996155	0.6226096155386671
0.689813625067	6.01435067712	-10.848129114089977
0.646357171949	5.79531694574	-7.535723277726625
0.603153745	5.56737224341	-4.223317441363274
0.558102688292	5.34260847179	-0.9109116049999221

$$0.514959956987 \quad | \quad 5.07329868242 \quad | \quad 2.4014942313634298$$

$\Delta E_{\text{Volmer}} / \text{eV}$	$\bar{\Phi} / \text{eV}$	$\frac{\overline{q}_{\text{exp}} + \overline{q}_{\text{imp}}}{A} / \mu\text{C cm}^{-2}$
0.413841084168	5.45765	5.8266235333340495
0.232051412662	4.9584	7.3400322432909455
0.0432996742747	4.3851	8.853440953247842
-0.1410884464	3.7734	10.36684966320474
-0.31470211713	3.1619	11.880258373161636
0.906838522791	5.63425	2.9133117666670247
0.802680585854	5.34565	3.6700161216454728
0.691814566293	5.0264	4.426720476623921
0.577374433356	4.68915	5.18342483160237
0.461897614678	4.34555	5.940129186580818
1.10503628531	5.8505	1.4566558833335124
1.05101780837	5.70375	1.8350080608227364
0.995422465683	5.5461	2.2133602383119606
0.937583068087	5.3818	2.591712415801185
0.889163911859	5.2121	2.970064593290409
1.00885672648	5.7751	1.942207844444683
0.941590998984	5.5837	2.4466774144303156
0.870267713821	5.37485	2.9511469844159475
0.79601573533	5.1519	3.4556165544015793
0.719870898858	4.92015	3.960086124387212
0.413839689583	5.4577	5.8266235333340495
0.232049303777	4.95845	7.3400322432909455
0.0433002185036	4.3851	8.853440953247842
-0.14108569125	3.77335	10.36684966320474

-0.31470051846	3.16185	11.880258373161636
-0.310761602446	4.54255	11.766752719914868
-0.41748400834	4.2351	12.523457074893317
-0.519474082263	3.92145	13.280161429871765
-0.615820480911	3.6061	14.03686578485021
-0.706223504891	3.2947	14.793570139828661
-0.64176007385	3.91245	14.736817313205277
-0.683218761871	3.76175	15.115169490694502
-0.723228851806	3.61175	15.493521668183725
-0.761750274913	3.46165	15.871873845672948
-0.798805276449	3.3118	16.250226023162174
-0.514855119713	4.1214	13.746795782108473
-0.577191300734	3.91815	14.251265352094103
-0.63700702721	3.714	14.755734922079737
-0.69419852172	3.51005	15.26020449206537
-0.748686769221	3.3074	15.764674062051002

Figure 7

POSCAR file corresponding to high work function case:

Pt H O

1.000000000000000

8.463839999999994 0.000000000000000 0.000000000000000

0.000000000000000 4.886599999999996 0.000000000000000

0.000000000000000 0.000000000000000 32.104089999999993

Pt H O

18 33 16

Selective dynamics

Direct

0.0000000000000000 0.0833333300000021 0.2180407600000009 F F F
0.3333333300000021 0.0833333300000021 0.2180407600000009 F F F
0.6666666699999979 0.0833333300000021 0.2180407600000009 F F F
0.1666666699999979 0.5833333300000021 0.2180407600000009 F F F
0.5000000000000000 0.5833333300000021 0.2180407600000009 F F F
0.8333333300000021 0.5833333300000021 0.2180407600000009 F F F
0.1666666699999979 0.2500000000000000 0.2897937799999966 F F F
0.5000000000000000 0.2500000000000000 0.2897937799999966 F F F
0.8333333300000021 0.2500000000000000 0.2897937799999966 F F F
0.3333333300000021 0.7500000000000000 0.2897937799999966 F F F
0.6666666699999979 0.7500000000000000 0.2897937799999966 F F F
0.0000000000000000 0.7500000000000000 0.2897937799999966 F F F
0.9985927700000019 0.4220822600000034 0.3635304200000036 F F F
0.3321781400000035 0.4215228600000032 0.3622850900000003 F F F
0.6658156000000020 0.4204424099999997 0.3622405099999995 F F F
0.1662878400000025 0.9220588900000024 0.3627106799999993 F F F
0.4995918899999978 0.9204650699999988 0.3628199999999993 F F F
0.8328582099999977 0.9209683999999996 0.3623438099999987 F F F
0.0294431399999979 0.2691702600000028 0.4674948400000005 F F F
0.9653096400000010 0.4541662000000031 0.4291165899999996 F F F
0.8369284199999996 0.4285194400000023 0.4730057299999970 F F F
0.4273882600000007 0.9438308000000006 0.4723800299999965 F F F
0.5432503899999972 0.9345016600000022 0.4348752300000029 F F F
0.1040323000000001 0.8282137500000033 0.4717710199999985 F F F
0.1736816100000027 0.9956579899999980 0.4352335800000020 F F F
0.6313659599999966 0.2664434599999979 0.4787605400000032 F F F

0.6326563499999978 0.5968401399999976 0.4790003100000035 F F F
 0.2230424164804887 0.8174671687320512 0.6253580176131806 T T T
 0.2183087201808362 0.1308833715906985 0.6179862456189582 T T T
 0.7803600767029408 0.8328237258925526 0.5926057183335232 T T T
 0.8379228673890040 0.8003522585512002 0.5469894285181809 T T T
 0.6193300819466430 0.7731053739773941 0.6518156274972142 T T T
 0.5051857300806901 0.8994517115181750 0.6193574696520372 T T T
 0.9923591213015612 0.1679255784063045 0.5807113540913349 T T T
 0.0012151876370439 0.4856132571032319 0.5849655036965515 T T T
 0.8837731503892101 0.1440339783154911 0.7891641525153545 T T T
 0.8323818213753995 0.2303733969091297 0.7448038184587702 T T T
 0.3055625819726941 0.8001825546997807 0.7324575755137417 T T T
 0.3537219750333094 0.9252066906454459 0.6899294023110443 T T T
 0.0566600916190225 0.5218182858781404 0.7571973231186533 T T T
 0.0467066157364258 0.8448947186022835 0.7572548530839995 T T T
 0.5220621282901092 0.2049722065995141 0.7331325798659449 T T T
 0.5309198441659433 0.5210487520578013 0.7260655694049092 T T T
 0.1800494947239386 0.9366093147138770 0.8669044249580651 T T T
 0.0172318583777837 0.0883463101593165 0.8663441918502812 T T T
 0.4890932959893064 0.5627292438530134 0.8362092637478753 T T T
 0.5942198452242380 0.4972362504333603 0.7977762235164718 T T T
 0.2216958743420037 0.4205512979580845 0.8539078144155710 T T T
 0.2218318743270231 0.6198076950613114 0.8156941944582599 T T T
 0.7275611348346729 0.8934273980524523 0.8364787604590234 T T T
 0.7182641266705474 0.2137221452098998 0.8418962785541098 T T T
 0.9655009299999975 0.4408172799999974 0.4616855200000032 F F F
 0.5409236300000018 0.9361776699999993 0.4662140300000033 F F F

0.1583247100000023 0.0016056600000027 0.4663059100000027 F F F
 0.6924818000000030 0.4309913499999993 0.4876129100000028 F F F
 0.2841926169003557 0.9835360938372801 0.6300662091402671 T T T
 0.8776301853482806 0.8320065348132957 0.5750033418506320 T T T
 0.6089906879688129 0.8107522096525699 0.6221956843579832 T T T
 0.0670853880800522 0.3202319145451398 0.5848475065411236 T T T
 0.9273017658310749 0.1846226843552188 0.7608212833321062 T T T
 0.3990955440866131 0.8628659392383966 0.7164027856266770 T T T
 0.1213718730848754 0.6899100832259037 0.7579958131191589 T T T
 0.5922365779253411 0.3643079406086827 0.7362794802111381 T T T
 0.1301099156004426 0.1158511400274307 0.8714235397231249 T T T
 0.6012572812392349 0.5479201970918908 0.8273101221137296 T T T
 0.2708827020942621 0.5921866361633334 0.8430625635146285 T T T
 0.7924758479154761 0.0609026289769332 0.8373697223640235 T T T

INCAR file corresponding to high work function case:

INCAR created by Atomic Simulation Environment

ENCUT = 500.000000

SIGMA = 0.050000

EDIFF = 1.00e-04

EDIFFG = -5.00e-02

PREC = Accurate

GGA = RP

ALGO = Normal

ISMEAR = 0

NELM = 250

IBRION = 2

NSW = 0
NCORE = 16
KPAR = 14
LWAVE = .FALSE.
LVHAR = .TRUE.
LDIPOL = .TRUE.
IDIPOL = 3
DIPOL = 0.5 0.5 0.5

POSCAR file corresponding to low work function case:

Pt H O
1.00000000000000
8.463839999999994 0.000000000000000 0.000000000000000
0.000000000000000 4.886599999999996 0.000000000000000
0.000000000000000 0.000000000000000 32.104089999999993
Pt H O
18 33 16
Selective dynamics
Direct
0.000000000000000 0.083333300000021 0.2180407600000009 F F F
0.333333300000021 0.083333300000021 0.2180407600000009 F F F
0.666666699999979 0.083333300000021 0.2180407600000009 F F F
0.166666699999979 0.583333300000021 0.2180407600000009 F F F
0.500000000000000 0.583333300000021 0.2180407600000009 F F F
0.833333300000021 0.583333300000021 0.2180407600000009 F F F
0.166666699999979 0.2500000000000000 0.2897937799999966 F F F
0.500000000000000 0.2500000000000000 0.2897937799999966 F F F

0.8333333300000021 0.2500000000000000 0.2897937799999966 F F F
 0.3333333300000021 0.7500000000000000 0.2897937799999966 F F F
 0.666666669999979 0.7500000000000000 0.2897937799999966 F F F
 0.0000000000000000 0.7500000000000000 0.2897937799999966 F F F
 0.9985927700000019 0.4220822600000034 0.3635304200000036 F F F
 0.3321781400000035 0.4215228600000032 0.3622850900000003 F F F
 0.6658156000000020 0.420442409999997 0.362240509999995 F F F
 0.1662878400000025 0.9220588900000024 0.362710679999993 F F F
 0.499591889999978 0.920465069999988 0.362819999999993 F F F
 0.832858209999977 0.920968399999996 0.3623438099999987 F F F
 0.029443139999979 0.2691702600000028 0.4674948400000005 F F F
 0.9653096400000010 0.4541662000000031 0.4291165899999996 F F F
 0.836928419999996 0.4285194400000023 0.4730057299999970 F F F
 0.4273882600000007 0.9438308000000006 0.4723800299999965 F F F
 0.5432503899999972 0.9345016600000022 0.4348752300000029 F F F
 0.1040323000000001 0.8282137500000033 0.4717710199999985 F F F
 0.1736816100000027 0.995657989999980 0.4352335800000020 F F F
 0.6313659599999966 0.2664434599999979 0.4787605400000032 F F F
 0.6326563499999978 0.5968401399999976 0.4790003100000035 F F F
 0.0473569091147468 0.5338370179183158 0.5809194215471081 T T T
 0.1889886844896296 0.5297858083191400 0.6115497494065565 T T T
 0.5430035023188680 0.0168740505087968 0.5703461172756690 T T T
 0.7086472968390325 0.1628669089715586 0.5765965883073321 T T T
 0.2781619322176994 0.2063204249692205 0.5624837339490796 T T T
 0.2726418274264901 0.8849283535798165 0.5645740414386466 T T T
 0.8133407959159129 0.4901159208966988 0.6167188784944742 T T T
 0.7734129257030986 0.6618154907481539 0.5775421773971701 T T T

0.0801144221247085 0.4213709675259310 0.7255804654487576 T T T
 0.9656228386657304 0.4399405195563730 0.6872411315744600 T T T
 0.4765223687674691 0.9537572764490889 0.6734924166530121 T T T
 0.6005453885777072 0.9747321360002985 0.6365255872375783 T T T
 0.1884120489146497 0.7608032249798171 0.6884832064667776 T T T
 0.1865579700190736 0.0852281180880041 0.6874104264436767 T T T
 0.6927687048179934 0.3015780683908673 0.6759640971063590 T T T
 0.6961459419479397 0.6293342131194919 0.6764728744331734 T T T
 0.1550936927126330 0.2268186408750665 0.7863895138082455 T T T
 0.9927499836018612 0.3852950173375973 0.7936940419594123 T T T
 0.5045775806241792 0.8719849122523939 0.7918430751324621 T T T
 0.6651276487319180 0.0317088531839644 0.7984368915495850 T T T
 0.2238919837867996 0.7406238701006629 0.7853587889874376 T T T
 0.2824663387800257 0.9153729161700142 0.7480500081139922 T T T
 0.7783141930449347 0.3759959697832400 0.8428437513460239 T T T
 0.7201580249324095 0.5501325481574995 0.8052429406554751 T T T
 0.965500929999975 0.4408172799999974 0.4616855200000032 F F F
 0.5409236300000018 0.9361776699999993 0.4662140300000033 F F F
 0.1583247100000023 0.0016056600000027 0.4663059100000027 F F F
 0.6924818000000030 0.4309913499999993 0.4876129100000028 F F F
 0.1649603478594912 0.5429588908375536 0.5819721948590839 T T T
 0.6499906775593445 0.9936230620964039 0.5828083419479597 T T T
 0.3422148253165744 0.0407906113171705 0.5586193553233656 T T T
 0.8347622669663437 0.5000383698632120 0.5864408347831258 T T T
 0.0795608580705434 0.4301105721201921 0.6946597630459124 T T T
 0.5903897852388766 0.9664009635697610 0.6675225078555442 T T T
 0.2561744171152895 0.9250863952254207 0.6915133162554596 T T T

```

0.7621903429536729 0.4635696262664908 0.6729873885398518 T T T
0.1004875051435619 0.4037465337082438 0.7821832798600923 T T T
0.6184006921380600 0.8481870534537990 0.7973289111624737 T T T
0.2831748126168350 0.9093287842727946 0.7790138576754799 T T T
0.7801133992393545 0.3794108480257492 0.8125640314776490 T T T

```

INCAR file corresponding to low work function case:

INCAR created by Atomic Simulation Environment

ENCUT = 500.000000

SIGMA = 0.050000

EDIFF = 1.00e-04

EDIFFG = -5.00e-02

PREC = Accurate

GGA = RP

ALGO = Normal

ISMEAR = 0

NELM = 250

IBRION = 2

NSW = 0

NCORE = 16

KPAR = 14

LWAVE = .FALSE.

LVHAR = .TRUE.

LDIPOL = .TRUE.

IDIPOL = 3

DIPOL = 0.5 0.5 0.5

Figure 8

Data corresponding to Figure 8:

$2\Delta E_{\text{CO}}$ (Lin. Mod. PB) / eV	Facet	q / $\mu\text{C cm}^{-2}$	$\bar{\Phi}$ / eV
-1.4563549651975336	211	-25.563257651181587	2.4116999999999997
-1.3756121224760136	211	-19.17244323838619	2.9161
-1.3285761570114119	211	-12.781628825590793	3.2227
-1.3215146668408124	211	-6.390814412795397	3.66655
-1.3133663539992995	211	0.0	4.07425
-1.1604698058217764	100	-15.654234352173216	2.99235
-1.119176802916627	100	-11.740675764129913	3.30785
-1.0760934950449155	100	-7.827117176086608	3.6059
-1.034064628292981	100	-3.913558588043304	3.88545
-0.9888406688842224	100	0.0	4.1495

$2\Delta E_{\text{CO}}$ (Planar CC) / eV	Facet	q / $\mu\text{C cm}^{-2}$	$\bar{\Phi}$ / eV
-1.4557301237909996	211	-25.563257651181587	2.5985500000000004
-1.3760662804706953	211	-19.17244323838619	3.04835
-1.3269396643881919	211	-12.781628825590793	3.3169
-1.3205175737093668	211	-6.390814412795397	3.7104
-1.313004374565935	211	0.0	4.0753
-1.1610345100634731	100	-15.654234352173216	3.1329000000000002
-1.122760542173637	100	-11.740675764129913	3.41075
-1.0815117577731144	100	-7.827117176086608	3.6702
-1.037887623642746	100	-3.913558588043304	3.91815
-0.9956928354804404	100	0.0	4.15185

$2\Delta E_{\text{CO}}$ (Mod. PB) / eV	Facet	q / $\mu\text{C cm}^{-2}$	$\bar{\Phi}$ / eV
-1.1557542090595234	100	-15.654234352173216	3.07875

-1.1162746408081148	100	-11.740675764129913	3.3621499999999997
-1.075886484439252	100	-7.827117176086608	3.63065
-1.03174220470828	100	-3.913558588043304	3.89095
-0.9893668690201594	100	0.0	4.15075
-1.4118651689204853	211	-22.367850444783887	2.8058
-1.3731766355922446	211	-19.17244323838619	3.02855
-1.3273621211192221	211	-12.781628825590793	3.28355
-1.3215508579851303	211	-6.390814412795397	3.68225
-1.3137836405694543	211	0.0	4.0732